Biophysical Journal, Volume 99

**Supporting Material**

# Quantitative guidelines for force calibration through spectral analysis of magnetic tweezers data

Aartjan J.W. te Velthuis, Jacob W.J. Kerssemakers, Jan Lipfert, and Nynke H Dekker

**Supplemental information for:**

# Quantitative guidelines to force calibration through spectral analysis of magnetic tweezers data

Aartjan J. W. te Velthuis, Jacob W. J. Kerssemakers, Jan Lipfert, and Nynke H. Dekker.

**Supplemental text**

***1. Sampling time vs. measurement error***

Both the time for which we simulate our magnetic tweezers experiments and how long we sample real data with a CCD camera influence the statistical uncertainty in any force measurement (1). How long should we thus measure to get a proper force measurement, assuming we take into account an expected or target force $F$, a DNA extension $L_{ext}$ and a, for example, 10% acceptable statistical error? We assume we measure N points during time T. Since these points should be independent, they need to be taken at least one relaxation time $\tau$ apart, i.e. $N = T / \tau$. For the $x$-direction, this relaxation time is

$$\tau = \frac{\gamma}{k_x} = \frac{12\pi^2 \eta R_0 L_{ext}}{F} \qquad [1]$$

Starting from equation 8 of the main manuscript, the error can be deduced from:

$$F = \frac{k_B T L_{ext}}{\langle \delta x^2 \rangle} \qquad [2]$$

The associated error propagation can then be described as:

$$\frac{\delta F}{F} = \sqrt{\left[\frac{\delta L_{ext}}{L_{ext}}\right]^2 + \left[\frac{\delta \langle \delta x^2 \rangle}{\langle \delta x^2 \rangle}\right]^2} \qquad [3]$$

In the magnetic tweezers, the DNA extension $L_{ext}$ depends on the force applied in the $z$-direction. Since we measure both $L_{ext}$ and the fluctuations of the signal over $N$ sampling points with a certain standard error $\sigma$, we obtain:

$$\left[\frac{\delta L_{ext}}{L_{ext}}\right]^2 = \frac{{\sigma_z}^2}{N{L_{ext}}^2} \qquad [4]$$

and

$$\left[\frac{\delta\left\langle \delta x^2 \right\rangle}{\left\langle \delta x^2 \right\rangle}\right]^2 = \left[\frac{{\sigma_x}^2 / N}{{\sigma_x}^2}\right]^2 = 1/N^2 \qquad [5]$$

where

$\sigma^2{}_x = k_B T / k_x$ and $\sigma^2{}_z = k_B T / k_z$

with $k_B$, $T$ and the stiffnesses as defined in the main text with equations 5 and 7. When we combine equations 3-5 this subsequently gives:

$$\frac{\delta F}{F} = \sqrt{\frac{{\sigma_z}^2}{N{L_{ext}}^2} + \frac{1}{N^2}} = \frac{1}{N}\sqrt{N.\left[\frac{\sigma_z}{L_{ext}}\right]^2 + 1} \qquad [6]$$

Using $k_z(F) = \left.\frac{\delta F_{WLC}}{\delta z}\right|_F$ [7]

We obtain:

$$\frac{\delta F}{F} = \frac{1}{\sqrt{N}}\sqrt{\frac{k_B T}{{L_{ext}}^2}\left[\frac{\delta F_{WLC}}{\delta z}\right]^{-1} + 1} \qquad [8]$$

This relationship allows us to determine the number of independent sample points $N$ as function of $F$, given a desired accuracy $\frac{\delta F}{F} = \varepsilon$. We deduce that:

$$N = \frac{1}{\varepsilon^2}\left(\frac{k_B T}{{L_{ext}}^2}\left[\frac{\delta F_{WLC}}{\delta z}\right]^{-1} + 1\right) \qquad [9]$$

which can be reexpressed in terms of the sampling time:

$$T = \tau \cdot \frac{1}{\varepsilon^2} \cdot \left( \frac{k_B T}{L_{ext}^2} \left[ \frac{\delta F_{WLC}}{\delta z} \right]^{-1} + 1 \right)$$

Substituting $\tau$ equation 1, we obtain our final expression:

$$T = \frac{1}{\varepsilon^2} \frac{12\pi^2 \eta R_0 L_{ext}}{F} \cdot \left( \frac{k_B T}{L_{ext}^2} \left[ \frac{\delta F_{WLC}}{\delta z} \right]^{-1} + 1 \right) \qquad [10]$$

As a rule of thumb, the first term between brackets expresses the contribution from the uncertainty in $L_{ext}$. This term approaches unity for short (<1 micron) tethers at low forces (<0.1 pN) and $N$ has to be >100 for $\varepsilon = 0.1$.

***2. Tracking error***

If we measure the bead positions with a certain tracking error $\sigma_T$ and variance $\sigma^2{}_T$. Sampling $N$ points will therefore result in an additive error in force measurements, giving:

$$F' = \frac{k_B T L_{ext}}{\sigma^2 + \sigma_T{}^2} \qquad [11]$$

Thus,

$$\frac{F' - F}{F} = \frac{F'}{F} - 1 = \frac{\sigma^2}{\sigma^2 + \sigma_T{}^2} - 1 = \frac{1}{\sigma^2 / \sigma_T{}^2 + 1} \qquad [12]$$

This thus amounts to a bias $\varepsilon_T$ in the force:

$$\varepsilon_T = 1 \cdot \left( \frac{k_B T L_{ext}(F)}{F \cdot \sigma_T{}^2} + 1 \right)^{-1} \qquad [13]$$

**3. Corrections to the bulk viscosity in proximity of the surface**

In the proximity of the flow cell surface, the Stokes drag on the tethered bead increases (2). This increase becomes significant once the distance $z$ to the surface reaches the same order of magnitude as the bead's radius, as described by Happel and Brenner (3). If one continues to use the bulk viscosity ($\eta$) contribution to the drag mathematically, the measurement bead radius ($R_m$) will appear larger than the expected radius $R_0$ by the viscosity correction factor $C_\eta$:

$$R_m = R_0 \cdot C_\eta \qquad [14]$$

where

$$C_\eta(z,R) = \left[1 - \frac{9}{16}\left(\frac{R}{L_{ext}}\right) + \frac{1}{8}\left(\frac{R}{L_{ext}}\right)^3 - \frac{45}{256}\left(\frac{R}{L_{ext}}\right)^4 - \frac{1}{16}\left(\frac{R}{L_{ext}}\right)^5\right]^{-1} \qquad [15]$$

Use of $R_m$ in the computation of the system's cut-off frequency (see equation 11 of the main text) would lead to an erroneous value. To recover the correct $R_0$, we compute:

$$R_0 = \frac{R_m}{C_\eta} \approx R_m \cdot \left[1 - \frac{9}{16}\frac{R_0}{z}\right] \Leftrightarrow R_0 = R_0 \cdot \left[1 + \frac{9}{16}\frac{R_m}{z}\right]^{-1} \qquad [16]$$

where we have ignored quadratic and higher-order terms. However, in our bead tracking procedure we do not directly observe $z$ (the distance to the surface), but the height difference (extension) between the tethered bead and a reference bead (Fig. 1A). If we assume that these have the same radius, we can transform equation 16 accordingly and solve it to yield $R_0$ as a function of $R_m$ and $L_{ext}$:

$$R_0 = \frac{1}{2}\left[\left(\frac{7}{16}R_m - L_{ext} + \sqrt{(\frac{7}{16}R_m - L_{ext})^2 + 4L_{ext}R_m}\right)\right] \qquad [17]$$

**4. Camera integration window**

Sampling Brownian motion with a camera results in two effects. The first is time averaging or motion blur, which leads to suppression of the signal. The experimentally measured variance $\mathrm{var}(x_m)$ is therefore lower than the true variance that is required for precise force calibration (Fig. 3B main text). The second is aliasing, which results in a contribution to the frequencies of the measured spectrum by signals that are higher than the sampling frequency. This principle is also known as back-folding, and although it does not affect the power of the spectrum it does change its shape, and consequently the cut-off frequency of the system. In the following section, we will discuss how we can correct for these effects in the spectral domain.

If we assume that the integration window of the camera is rectangular (Fig. 3A main text), we can define the relation between the measured bead position $x_m(t)$ and the true bead position $x(t)$ as:

$$x_m(t) = \int_{t-W}^{t} x(t')\mathrm{H}(t-t')\,dt' \qquad [18]$$

where $\mathrm{H}(t)$ is defined as:

$$\mathrm{H}(t) = \begin{cases} \dfrac{1}{W} & 0 < t \le W \\ 0 & \textit{Elsewhere} \end{cases} \qquad [19]$$

The power spectrum of the moving average window $P_{window}(\omega)$ is given by:

$$\mathrm{P}_{window}(\omega) = \left( \frac{\sin(\omega W/2)}{\omega W/2} \right)^2 \qquad [20]$$

Convolution of this spectrum with the spectrum of the tethered bead (see main text, equation 10) yields an expression for the measured variance:

$$\mathrm{var}(x_m) = \frac{1}{2\pi}\int \mathrm{P}(\omega)\mathrm{P}_{window}(\omega)\, d\omega \qquad [21]$$

**Supplemental references**


1. Strick, T. 1999. Mechanical supercoiling of DNA and its relaxation by topoisomerases. PhD thesis. University of Paris VI, Paris.
2. Schäffer, E., S. F. Norrelykke, and J. Howard. 2007. Surface forces and drag coefficients of microspheres near a plane surface measured with optical tweezers. Langmuir 23:3654-3665.
3. Happel, J., and N. Brenner. 1965. Low reynolds number hydrodynamics with special application to particulate media. Prentice-Hall, Englewood Cliffs, N.J.

**Supplemental tables**

Table S1

| **Parameter settings** | **Parameter value** |
|---|---|
| Viscosity | 0.001 kg/m*s |
| Force | 0.01-10 pN |
| Bead radius | 1.4 µm |
| Contour length | 2.7 µm |
| Persistence length | 50 nm |
| Simulation time step | 0.005 ms |
| Sampling frequency | 120 Hz |
| Shutter time | 8.33 ms |

Table S2

| **Camera correction** | **Bead radius** (µm) | **Viscosity (kg/m*s)** | **Sampling frequency (Hz)** | **Increase in F (error 10%)** | **Relative increase in F (error 10%)** |
|---|---|---|---|---|---|
| No | 0.5 | 0.001 | 120 | - | - |
| Yes | 0.5 | 0.001 | 120 | $1.4 \pm 0.05$[a] | - |
| Yes | 0.5 | 0.001 | 200 | $1.5 \pm 0.03$[b] | $0.9 \pm 0.03$[b] |
| Yes | 1.4 | 0.001 | 120 | $2.8 \pm 0.04$[b] | $1.0 \pm 0.04$[b] |
| Yes | 0.5 | 0.002 | 120 | $2.0 \pm 0.05$[b] | $1.0 \pm 0.05$[b] |

a: relative to spectral analysis without camera correction
b: relative to spectral analysis with camera correction

**Supplemental figures**

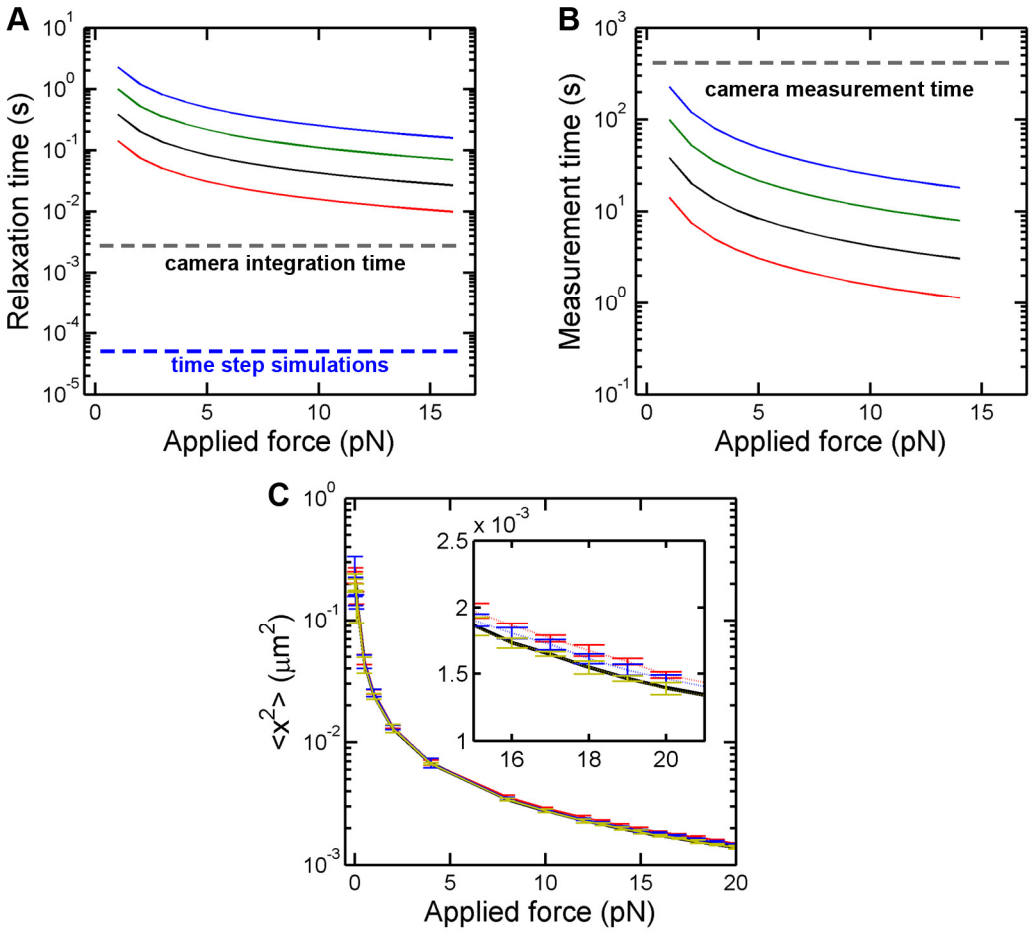


**Fig. S1. Time scales in the simulation.** (**A**) Simulations showing the relaxation times in the magnetic tweezers for tethered systems of different contour lengths ($L_0$ = 16 µm, blue; $L_0$ = 7 µm, green; $L_0$ = 2.7 µm, black; $L_0$ = 1 µm, red) as a function of the input applied force. The dashed blue line indicates the simulation time step employed in the simulations of magnetic tweezers data, whereas the dashed grey line indicates the integration time of the camera. Traces were generated with parameters $R$ = 1.4 µm for the bead and $L_p$ = 50 nm for the persistence length of the tether. (**B**) Simulations showing the required time durations for accurate measurement (<10% statistical error; see also

supplemental text) of the force in the magnetic tweezers for tethered systems of different contour lengths as in Fig. S1A. The dashed grey line indicates the overall measurement time by the camera (i.e. 5 min). (**C**) The simulated bead variances obtained with different simulation time steps ($\Delta t$ = 0.05 ms, red; $\Delta t$ = 0.01 ms, blue; $\Delta t$ = 0.005 ms, yellow; theoretical deviations, black line) plotted against the applied simulated force. Overall, we observe no significant dependence of the simulated variances on the size of the time step in the range investigated. Only for the highest forces, do we observe that long simulation time steps lead to a small deviation from the theoretical relation between the force and the bead displacement (equation 2), see inset. In practice, we employ a time step $\Delta t$ = 0.005, which provides a good approximation to the theoretical curve.

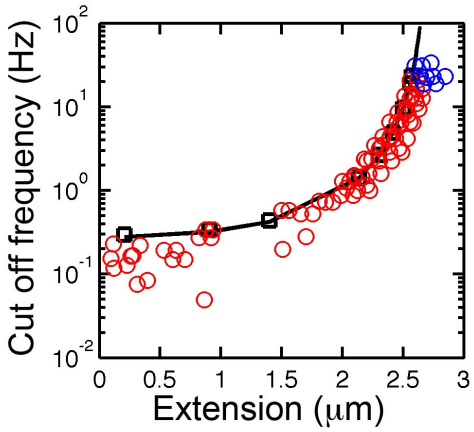


**Fig. S2. Cut-off frequencies for experimental 7.9 kb DNA**. Cut off frequencies obtained after spectral analysis as function of the tether extension. Simulated data is indicated in black squares, whereas experimental data is represented as red circles. Indicated in blue are the data points that lie outside the inextensible WLC fit (see main text, Fig. 7A).

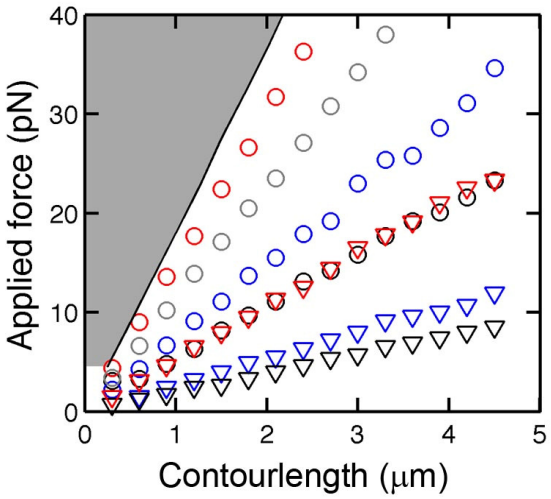


**Fig. S3. Limits in the estimation of the force and a 5 nm tracking error**. DNA constructs tethered to beads with a radius of 1.4 μm (circles) or a radius of 1 μm (triangles) were used to create 10% error plots under varying conditions. Curves are shown for uncorrected spectral analysis (black), camera-corrected analysis (blue), camera-corrected analysis for traces simulated at a two-fold higher viscosity (red), and camera-corrected analysis for traces sampled at 200 Hz instead of 120 Hz (grey). Indicated by the black line is the force that can maximally be measured with 10% accuracy when the tracking error of the camera is 5 nm. The grey-shaded area represents force measurements with tracking errors <5 nm.

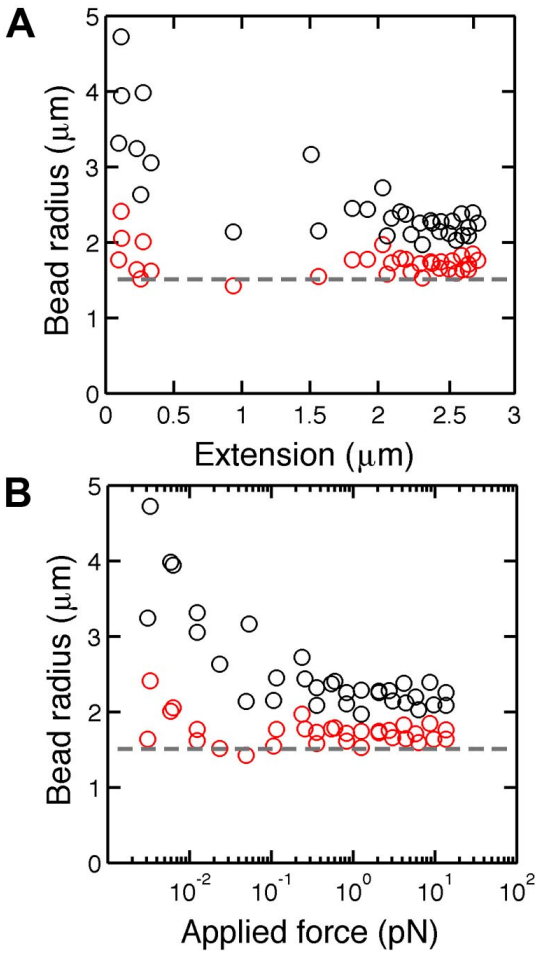


**Fig. S4. Bead radius estimation in the presence or absence of viscosity corrections**. (**A**) Bead radii extracted from experimental data following spectral analysis, plotted as function of the extension of the tether. As shown, when the spectral analysis is performed in the absence (black circles), the estimated bead radius is significantly larger than the bead radius used for the experiment. When the spectral analysis is performed in the presence (red circles) of viscosity corrections, a much better estimation of the bead radius is obtained. According to the manufacturer, the beads employed had a radius of ~1.4 μm (indicated by the grey dotted line). The dsDNA tether used had a contour length of 2.7 μm. (**B**) Bead radii extracted from experimental data following spectral analysis, plotted as function of the applied force. As the results of the spectral analysis demonstrate, the

viscosity correction (black circles) allows us to recover the correct bead radius at all forces except forces below 0.001pN. When the spectral analysis is performed in the absence (red circles) of viscosity corrections, however, the estimation of the bead radius is significantly larger at all forces. This procedure is not only illustrates the necessity of applying viscosity corrections at low and relatively high forces, it also shows how the bead radius can be used to check the performance of the spectral analysis. As in (A), the beads employed had a radius of ~1.4 μm (indicated by the grey dotted line).